

## Experimental Demonstration of the Effectiveness of Electromagnetically Induced Transparency for Enhancing Cross-Phase Modulation in the Short-Pulse Regime

Greg Dmochowski,<sup>1,\*</sup> Amir Feizpour,<sup>1</sup> Matin Hallaji,<sup>1</sup> Chao Zhuang,<sup>1</sup> Alex Hayat,<sup>1,2</sup> and Aephraim M. Steinberg<sup>1,2</sup>

<sup>1</sup>*Centre for Quantum Information and Quantum Control, and Institute for Optical Sciences,*

*Department of Physics, University of Toronto, 60 St. George Street, Toronto, Ontario, Canada M5S 1A7*

<sup>2</sup>*Canadian Institute for Advanced Research, 180 Dundas Street West, Toronto, Ontario, Canada M5G 1Z8*

(Received 24 June 2015; published 28 April 2016)

We present an experiment using a sample of laser-cooled Rb atoms to show that cross-phase modulation schemes continue to benefit from electromagnetically induced transparency (EIT) even as the transparency window is made narrower than the signal bandwidth (i.e., for signal pulses much shorter than the response time of the EIT system). Addressing concerns that narrow EIT windows might not prove useful for such applications, we show that while the peak phase shift saturates in this regime, it does not drop, and the time-integrated effect continues to scale inversely with EIT window width. This integrated phase shift is an important figure of merit for tasks such as the detection of single-photon-induced cross-phase shifts. Only when the window width approaches the system's dephasing rate  $\gamma$  does the peak phase shift begin to decrease, leading to an integrated phase shift that peaks when the window width is equal to  $4\gamma$ .

DOI: 10.1103/PhysRevLett.116.173002

The interaction between individual photons is notoriously weak. This is an obstacle, for instance, to optical quantum computing; while the lack of interactions is helpful for coherent communications, it leaves the construction of deterministic logic gates between photonic qubits a difficult challenge.

Nonlinear optical properties of matter have been used to mediate an effective interaction between two optical fields. For example, an intensity-dependent refractive index provided by an atomic medium can lead to a conditional phase shift written on one optical “probe” field in the presence of a second “signal” field. This effective interaction serves as the basis for a two-photon gate proposal, which requires a  $\pi$  rad phase shift to be acquired by the probe field [1]. The difficulty of achieving such a large phase shift has prompted the proposal of a new approach that relies merely on the single-shot detectability of any observable cross-phase shift, not necessarily  $\pi$  rad [2]. However, even the nonlinearities required for this “weak nonlinearity” scheme are many orders of magnitude larger than those achievable in typical situations.

A number of approaches have been proposed for greatly enhancing the strength of cross-phase modulation (XPM), including cavity QED [3], unconventional media such as photonic crystal fibers [4] and hollow-core fibers filled with alkali gas [5], and, finally, novel physical effects such as electromagnetically induced transparency (EIT) [6,7]; this Letter addresses the latter.

The original “ $N$  scheme” proposed by Schmidt and Imamoglu [8] made use of a single EIT window, while later works investigated double- $\Lambda$  systems [9,10] to overcome limitations arising from the group-velocity mismatch between signal and probe pulses. Many variations on these

multilevel schemes have been introduced [11–16] and the ability to store light using EIT has even led to cross-phase modulation between stored pulses of light [17]. In the past 3 years, remarkably high nonlinearities have been observed relying on Rydberg blockade in the presence of EIT [18–21], presaging potentially huge cross-phase shifts.

The enhancement provided by EIT schemes arises from the spectral narrowness of the transparency window, which results in a steep refractive index profile for the probe field. The presence of the signal field introduces an ac Stark shift, which imprints a phase shift on the probe that is proportional to the slope of this refractive index profile. Meanwhile, the ac Stark shift is intensity dependent: a larger shift will be produced by compressing the signal energy into a temporally shorter pulse. Presumably, then, the largest nonlinear effect is achieved when spectrally narrow transparency windows are perturbed by short, intense signal pulses. However, reducing the spectral width of the transparency window  $\Delta_{\text{EIT}}$  implies a slower response time for the EIT medium. This suggests that a fundamental limitation may exist for EIT-enhanced XPM schemes; once the inverse EIT bandwidth  $1/\Delta_{\text{EIT}}$  exceeds the temporal width of the signal pulse  $\tau_s$  (i.e., once the signal pulse is shorter in time than the response time of the medium), the EIT medium may not respond quickly enough to provide a practical benefit. Theoretical [22,23] and experimental [24] investigations of step-function signal fields have, indeed, found that narrower windows, while providing a larger steady-state phase shift, require more time to reach this steady state. The authors went on to conclude that such a slow response time may be a limitation in the case of pulsed signal fields. However, there has been no study of the transient behavior of EIT-enhanced XPM in this practically

more relevant scenario where the signal is a (broadband) pulse. It has thus far been unclear whether the advantages of the original theoretical proposal [8] (which treated only the single-mode problem) hold in practice.

Here we show experimentally that narrow transparency windows continue to benefit XPM even when  $\tau_s \ll 1/\Delta_{\text{EIT}}$ . The slow dynamics reported for step responses [22–24] are actually at the root of the enhancement offered by EIT in the regimes of most practical interest, namely, narrow transparency windows perturbed by short, intense signal pulses. While the peak phase shift saturates when  $\tau_s \leq 1/\Delta_{\text{EIT}}$ , it does not decrease as  $\Delta_{\text{EIT}} \rightarrow 0$ , and the narrow EIT bandwidth serves to prolong the effect of the short signal pulse. As a result, we find that in the short-pulse regime, the integrated phase shift (though not the peak phase shift) continues to scale linearly with  $1/\Delta_{\text{EIT}}$ . For weak nonlinearity schemes [2], which rely on the mere detectability of a single-shot cross-phase shift (not necessarily  $\pi$  rad), this amounts to a significant advantage over non-EIT schemes. This work constitutes the first study of EIT-enhanced XPM in this experimentally relevant regime of spectrally narrow transparency windows perturbed by broadband signal pulses.

We study the effects of EIT on XPM using an ensemble of  $^{85}\text{Rb}$  atoms cooled and trapped in a magneto-optical trap (MOT). The level scheme, shown in Fig. 1, makes use of the two  $5^2S_{1/2}$  hyperfine ground states along with the  $5^2P_{3/2}$   $F' = 2$  excited state to form a three-level  $\Lambda$  system. When the probe and coupling fields satisfy the two-photon resonance condition (i.e., when their respective detunings are equal), the atomic medium is rendered transparent to the probe beam. The degree of transparency (as well as the refractive index) experienced by the probe beam depends strongly on its detuning from this two-photon resonance. Under EIT conditions, pulses of signal light blue detuned by 40 MHz from the  $F = 3 \rightarrow F' = 4$  transition are sent through the medium, ac Stark shifting the  $F = 3$  hyperfine ground state. This energy shift of the ground state changes

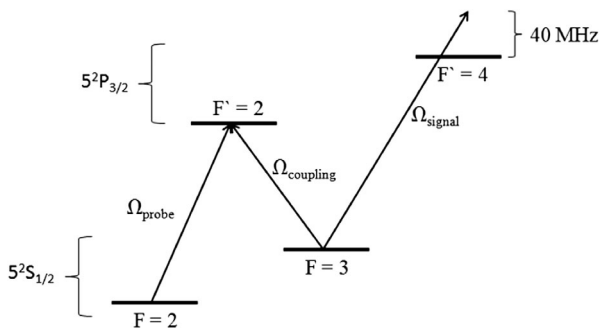


FIG. 1. Level scheme used to implement EIT enhanced XPM in  $^{85}\text{Rb}$  atoms. A probe beam ( $\Omega_{\text{probe}}$ ) addressing the  $5^2S_{1/2} \rightarrow 5^2P_{3/2}$  transition experiences EIT due to a strong coupling beam ( $\Omega_{\text{coupling}}$ ), while a detuned signal pulse ( $\Omega_{\text{signal}}$ ) serves to ac Stark shift the  $F = 3$  ground state, producing a cross-phase shift on the probe field.

the two-photon detuning, imprinting a phase shift on the probe field, which, in the steady state, is inversely proportional to the EIT window width.

The phase shift is measured using a beat-note interferometry [25] technique (the frequency-domain analog of a spatial interferometer). A “reference” beam, copropagating with the probe field but blue detuned by 100 MHz, is also sent into the medium, serving as a phase reference. This detuning is large enough that the phase shift imprinted on the reference beam due to the signal-induced ac Stark shift is negligible. The phase shift of the on-resonance probe field manifests itself as a phase shift of the resulting beat signal, which is read out by demodulation at 100 MHz. The coupling and signal fields also copropagate with these two probing fields, and all the beams are focused down to a beam waist of  $\approx 50 \mu\text{m}$  centered on the 2 mm diameter atomic cloud. After an initial 10 ms cooling time, the magnetic field gradient and trapping lasers are turned off for 1 ms, leaving only the cw probing and coupling fields on while pulses of signal light are sent into the medium. This cycle is repeated and every data point presented below corresponds to an average of several thousand pulses. The cloud of atoms has a density of  $\approx 10^{10} \text{ cm}^{-3}$ , and is cooled down to  $\approx 50 \mu\text{K}$ , with an optical density of 3 as seen by the on-resonance probe beam. We observed  $\approx 15\%$  atom number fluctuations from shot to shot throughout the experiment. The coupling and signal fields have the same polarization, which is orthogonal to the polarization of the probe fields, allowing for the detection of the probe alone.

Figure 2 shows temporal profiles of the cross-phase shift acquired by the probe beam due to a 40 ns (rms),  $0.8 \mu\text{W}$  peak power Gaussian signal pulse for a variety of EIT window widths. The spectral widths of the transparency windows were measured separately (by scanning the frequency of the probe laser across the two-photon

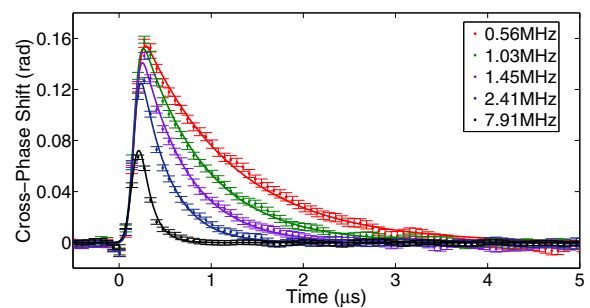


FIG. 2. Temporal profile of XPM for a variety of transparency window widths (as labeled in the legend). After the arrival of the 40 ns (rms) Gaussian signal pulse, the phase shift rises with a time scale given by the signal pulse duration, irrespective of  $\Delta_{\text{EIT}}$ . The decay is governed by the larger of  $\tau_s$  and  $1/\Delta_{\text{EIT}}$ . For  $1/\Delta_{\text{EIT}} > \tau_s$ , the phase returns to its original steady-state value at a rate given by  $\Delta_{\text{EIT}}$ . In addition, the peak phase shift saturates as the window width is narrowed. The fits to the data (solid lines) are obtained from a linear time-invariant system model of the interaction [26].

transition) and are listed in the legend; a ground state dephasing rate of 90 kHz was inferred from these window widths. The coupling beam powers ranged from 192 nW to 5  $\mu$ W depending on the desired EIT window width while the on- and off-resonance probe powers were kept at 8 and 100 nW, respectively, throughout. Each trace in Fig. 2 is an average of 2500 signal pulses. Contrary to step-response behavior, the rise of the phase shift is seen to be independent of the EIT window. While the peak phase shift saturates for small  $\Delta_{\text{EIT}}$ , it does not decrease and the effect of the signal pulse lasts longer for narrower windows. For example, in the case of a 0.56 MHz transparency window, the 40 ns signal pulse produces a phase shift that decays with a  $1/e$  time of 1.1  $\mu$ s.

The solid curves in Fig. 2 are fits to the data based on a linear time-invariant (LTI) model; in the cross-Kerr regime, we can abstract the underlying nonlinearity and treat the phase of the on-resonance probe field as the output of a linear system, which is being driven by the signal field intensity. This phase, then, is given by the convolution of the Gaussian signal pulse with the impulse response function of the EIT system, which can be well approximated by a decaying exponential with decay constant  $\tau$ . The result of the convolution yields the following expression for the time dependence of the nonlinear phase shift:

$$\phi(t) = \frac{\phi_0 n_s}{2\tau} e^{\tau_s^2/2\tau^2} e^{-t/\tau} \left[ 1 + \text{erf} \left( \frac{t}{\sqrt{2}\tau_s} - \frac{\tau_s}{\sqrt{2}\tau} \right) \right], \quad (1)$$

where  $\phi_0$  is the integrated phase shift per photon,  $n_s$  is the number of signal photons, and  $\tau_s$  is the rms duration of the signal pulse intensity. In a separate work [26], we have theoretically investigated the validity of this approach and found excellent agreement with a rigorous semiclassical treatment. When fitting, both the signal pulse duration  $\tau_s$  and the time constant of the decaying exponential  $\tau$  were left as free parameters (along with the magnitude of the shift and a horizontal offset); their quantitative agreement with the theoretically known values are discussed below.

Figure 3 plots the peak and integrated phase shifts, as extracted from Fig. 2, versus  $\Delta_{\text{EIT}}$  (note inverted scale). While single-mode as well as step-response treatments yield a linear dependence of phase shift on  $1/\Delta_{\text{EIT}}$ , the peak phase shift saturates in the presence of a broadband signal pulse as  $\Delta_{\text{EIT}}$  is narrowed (left to right in the figure). The vertical dashed lines in Fig. 3 denote the 2 MHz bandwidth of the signal pulse. We see, then, that the enhancement provided by narrow EIT windows saturates once the signal bandwidth exceeds that of the EIT system. For purposes of achieving  $\pi$  rad phase shifts, this clearly presents a limitation. The integrated phase shift, on the other hand, continues its linear growth far into the regime where the peak phase shift has saturated. Decreasing the EIT window by an order of magnitude causes the integrated phase shift to grow proportionally while the peak phase shift grows by

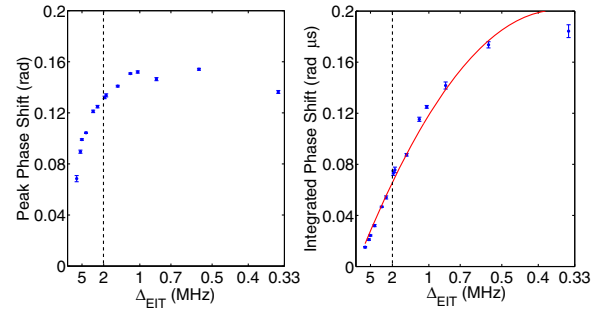


FIG. 3. Peak (left) and integrated (right) phase shifts as extracted from Fig. 2 plotted against EIT window width (note inverted scale). Decreasing the EIT window width by an order of magnitude results in an integrated phase shift that grows (nearly) proportionally while the peak phase shift saturates after increasing by a factor of 2. The vertical dashed line at 2 MHz corresponds to the bandwidth of the signal pulse. The deviation from linearity of the integrated phase shift occurs when the transparency window becomes comparable to the dephasing rate of the EIT system. The red curve is a fit to the data based on a linear time-invariant model.

only a factor of 2. In fact, it is only the finite coherence time of our system that disrupts the linear scaling of the integrated cross-phase shift with  $1/\Delta_{\text{EIT}}$  [26]. The dephasing in our system is due to lingering, inhomogeneous magnetic fields that persist during the measurement. As  $\Delta_{\text{EIT}}$  nears the dephasing rate  $\gamma$ , the peak phase shift will begin to drop, leading to an integrated phase shift that peaks when  $\Delta_{\text{EIT}} = 4\gamma$ .

The red curve in Fig. 3 is a fit to the data using an expression for the integrated phase shift as derived from the LTI model [26]. Based on separate measurements of EIT window widths, a dephasing of 90 kHz was assumed, leaving only a single free parameter, which agrees very well with the expected value given knowledge of the beam waist, detuning, optical density, and number of signal photons in the pulse. It should be noted that the optical density for the last data point in Fig. 3 (corresponding to  $\Delta_{\text{EIT}} = 0.34$  MHz) was 18% lower than the average optical density used in the remaining data points; this accounts for the anomalously lower value of the integrated phase shift for that window width.

Figure 3 shows that the original  $N$ -scheme proposal breaks down when we attempt to exploit both narrow EIT windows and broadband signal pulses. Given that the peak phase shift saturates, the linear growth of the integrated phase shift must be due to the longer duration of the effect. The temporal profile of the cross-phase shift [Eq. (1)] contains in it a dependence on both the signal pulse duration  $\tau_s$  and the EIT response time  $\tau$ . In the narrow EIT regime ( $\tau \gg \tau_s$ ), these can be regarded as the rise and fall times, respectively, of the cross-phase shift; for short times  $t$ , the error function term dominates, its time scale set by  $\tau_s$ , whereas for longer times the decaying exponential will take over with a time constant governed by the EIT system.



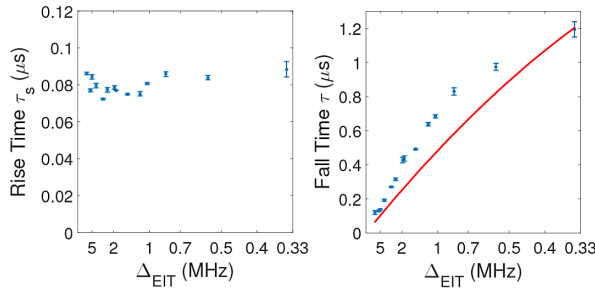


FIG. 4. Rise time  $\tau_r$  (left) and fall time  $\tau_f$  (right) of XPM plotted against EIT window width (note inverted scale) as extracted from fitting the data in Fig. 2 to Eq. (1). As the EIT window is narrowed, the decay of XPM is slower, while the rise time is unaffected, being given by a convolution of the measurement sampling period (67 ns) and the signal pulse duration (40 ns). The red line is a parameter-free theory curve, Eq. (2), describing the response time of the EIT medium.

Figure 4 plots the rise and fall times (i.e.,  $\tau_r$  and  $\tau_f$ , respectively) as extracted from the fits to Fig. 2. The roughly constant rise time of approximately 80 ns arises from the smearing out of the signal pulse duration (40 ns) by the measurement sampling period of 67 ns. The fall time, on the other hand, is seen to grow as the EIT window is narrowed. The presence of the signal pulse inside the medium disrupts the atomic coherence established by the probe and coupling fields. After the signal pulse passes, this coherence returns to its steady-state value on a time scale governed by the width of the EIT window. The lower field strengths necessary for narrow EIT windows yield a slower optical pumping rate back into the dark state, and, therefore, a longer time is needed to return to steady state. The red line in Fig. 4 is a theoretical curve (with no free parameters) for the fall time  $\tau$  of the phase shift:

$$\tau = \left[ 1 + \frac{d_0}{4} \left( 1 - \frac{2\gamma}{\Delta_{\text{EIT}}} \right) \right] \frac{2}{\Delta_{\text{EIT}}}. \quad (2)$$

This expression is introduced as the exponential rise time of cross-phase modulation in the case of a step-function signal field [22]. Since the impulse response is the derivative of the step response, Eq. (2) carries over as the decay constant  $\tau$  found in the exponential term of Eq. (1). We see, then, that the decay of the cross-phase shift in the wake of broadband signal pulses ( $\tau_r \ll 1/\Delta_{\text{EIT}}$ ) obeys the same dynamics as the step response of XPM. In both cases, a linear system is evolving toward a steady state—either returning to its original steady state upon passage of the signal pulse or progressing towards a new steady state in the presence of a step-function signal field. This is why we conclude that the slow dynamics reported for the step response of EIT enhanced XPM are actually at the root of the enhancement for pulsed-signal XPM when  $\tau_s \ll 1/\Delta_{\text{EIT}}$ . However, it is obvious that the theoretical curve in Fig. 4 systematically underestimates the observed

decay times. This discrepancy can be accounted for by noting the presence of magnetic sublevels, which have differing coupling strengths to the  $F' = 2$  excited state manifold. Since the atomic population was distributed among these sublevels, parallel  $\Lambda$  systems arose, with differing spectral widths. See Supplemental Material [27] for the details of how this results in observed fall times that are longer than those predicted by Eq. (2), which considers only a single  $\Lambda$  system.

We have experimentally demonstrated that narrow EIT windows continue to provide a benefit for cross-phase modulation schemes even when the signal pulse duration is much shorter than the inverse window width. While the peak phase shift saturates, the integrated phase shift continues to scale linearly with  $1/\Delta_{\text{EIT}}$ . With respect to signal pulse duration, there is no minimum acceptable EIT window width: the integrated phase shift will continue to increase as the window is narrowed, limited only by dephasing of the EIT system. The extended duration of the cross-phase shift afforded by narrow EIT windows allows for a longer measurement time, which can bring about a significant reduction in noise. This enhancement is very promising for all-optical quantum computing schemes, as well as other applications relying on the nonlinear effects of low-energy optical pulses. We have recently used this to observe the cross-phase modulation of a single, postselected photon on a coherent state probe field [28].

We would like to thank Tilman Pfau for helpful discussions and first raising the concern of using broadband signal pulses with narrow EIT windows, as well as Alan Stummer for continued technical support and John Howell for helpful discussions. This work was funded by NSERC, CIFAR, and QuantumWorks.

\*dmochow@physics.utoronto.ca

- [1] G. J. Milburn, *Phys. Rev. Lett.* **62**, 2124 (1989).
- [2] W. Munro, K. Nemoto, and T. Spiller, *New J. Phys.* **7**, 137 (2005).
- [3] Q. A. Turchette, C. J. Hood, W. Lange, H. Mabuchi, and H. J. Kimble, *Phys. Rev. Lett.* **75**, 4710 (1995).
- [4] N. Matsuda, R. Shimizu, Y. Mitsumori, H. Kosaka, and K. Edamatsu, *Nat. Photonics* **3**, 95 (2009).
- [5] V. Venkataraman, K. Saha, and A. L. Gaeta, *Nat. Photonics* **7**, 138 (2013).
- [6] K.-J. Boller, A. Imamoglu, and S. E. Harris, *Phys. Rev. Lett.* **66**, 2593 (1991).
- [7] M. Fleischhauer, A. Imamoglu, and J. Marangos, *Rev. Mod. Phys.* **77**, 633 (2005).
- [8] H. Schmidt and A. Imamoglu, *Opt. Lett.* **21**, 1936 (1996).
- [9] Z.-B. Wang, K.-P. Marzlin, and B. C. Sanders, *Phys. Rev. Lett.* **97**, 063901 (2006).
- [10] B.-W. Shiau, M.-C. Wu, C.-C. Lin, and Y.-C. Chen, *Phys. Rev. Lett.* **106**, 193006 (2011).
- [11] S. Rebić, D. Vitali, C. Ottaviani, P. Tombesi, M. Artoni, F. Cataliotti, and R. Corbalán, *Phys. Rev. A* **70**, 032317 (2004).

- [12] S. Li, X. Yang, X. Cao, C. Zhang, C. Xie, and H. Wang, *Phys. Rev. Lett.* **101**, 073602 (2008).
- [13] A. Joshi and M. Xiao, *Phys. Rev. A* **72**, 062319 (2005).
- [14] C. Ottaviani, D. Vitali, M. Artoni, F. Cataliotti, and P. Tombesi, *Phys. Rev. Lett.* **90**, 197902 (2003).
- [15] D. Petrosyan and G. Kurizki, *Phys. Rev. A* **65**, 033833 (2002).
- [16] Y. Guo, S.-S. Li, and L.-M. Kuang, *J. Phys. B* **44**, 065501 (2011).
- [17] Y.-F. Chen, C.-Y. Wang, S.-H. Wang, and I. A. Yu, *Phys. Rev. Lett.* **96**, 043603 (2006).
- [18] T. Peyronel, O. Firstenberg, Q.-Y. Liang, S. Hofferberth, A. V. Gorshkov, T. Pohl, M. D. Lukin, and V. Vuletić, *Nature (London)* **488**, 57 (2012).
- [19] O. Firstenberg, T. Peyronel, Q.-Y. Liang, A. V. Gorshkov, M. D. Lukin, and V. Vuletić, *Nature (London)* **502**, 71 (2013).
- [20] W. Chen, K. M. Beck, R. Becker, M. Gullans, M. D. Lukin, H. Tanji-Suzuki, and V. Vuletić, *Science* **341**, 768 (2013).
- [21] S. Baur, D. Tiarks, G. Rempe, and S. Dürr, *Phys. Rev. Lett.* **112**, 073901 (2014).
- [22] M. V. Pack, R. M. Camacho, and J. C. Howell, *Phys. Rev. A* **74**, 013812 (2006).
- [23] G. F. Sinclair, *Phys. Rev. A* **79**, 023815 (2009).
- [24] M. V. Pack, R. M. Camacho, and J. C. Howell, *Phys. Rev. A* **76**, 033835 (2007).
- [25] Y.-F. Chen, Y.-C. Liu, Z.-H. Tsai, S.-H. Wang, and I. A. Yu, *Phys. Rev. A* **72**, 033812 (2005).
- [26] A. Feizpour, G. Dmochowski, and A. M. Steinberg, *Phys. Rev. A* **93**, 013834 (2016).
- [27] See Supplemental Material at <http://link.aps.org/supplemental/10.1103/PhysRevLett.116.173002> for a detailed description of how these parallel  $\Lambda$  systems affect the measured window width and the corresponding decay time of XPM.
- [28] A. Feizpour, M. Hallaji, G. Dmochowski, and A. M. Steinberg, *Nat. Phys.* **11**, 905 (2015).